TRANSACTIONS OF THE INSTITUTE OF FLUID-FLOW MACHINERY

No. 139, 2018, 63–96

Paweł Ziółkowski*

A thermodynamic analysis of a gas-steam turbine incorporating a full model of a spray – ejector condenser

Department of Energy Conversion, Institute of Fluid Flow Machinery, Polish Academy of Sciences 80-231 Gdansk, Fiszera 14, Poland

Abstract

The specific issues that occur in the mathematical modelling of a spray-ejector condenser have been presented. The results of a thermodynamic analysis of a steam-gas turbine cycle have been obtained by computational flow mechanics code. The main aim of the spray-ejector condenser is simultaneously condensing steam and compressing CO_2 from the condensation pressure to about 100 kPa. Hence, the most important innovation of this steam-gas cycle emerges as the enhanced condensation, which is based on the nano-injection of cold water and a jet-powered compression of CO_2 performed in the spray-ejector condenser.

Keywords: Computational flow mechanics modelling; Two-phase ejector; Thermodynamic analysis; Numerical analysis

Nomenclature

A	–	surface area, m^2
$\mathbf{c}$	–	velocity in CFD approach, m/s
c	–	velocity in CFM approach, m/s

*Email adress: pziolkowski@imp.gda.pl

CFD	–	computational fluid dynamics
CFM	–	computational flow mechanics,
$\mathbf{D}$	–	diffusive stress tensor
$\mathbf{e}$	–	versor
e	–	specific total energy ($= u + \frac{p}{\rho} + zg + \frac{c^2}{2}$), J/kg
$\mathbf{f}$	–	force coming from the surface mechanism
g	–	gravitational acceleration, m/s^2
h	–	specific enthalpy, kJ/kg
$\mathbf{I}$	–	Gibbs unit tensor
k	–	flow losses in mixing chamber
l	–	specific work, kJ/kg
$\mathbf{n}$	–	unit vector normal to section
N	–	power, kW
$\dot{m}$	–	mass flow rate, kg/s
p	–	pressure, MPa
R	–	gas constant, kJ/(kgK)
$\mathbf{R}$	–	friction force
$\dot{Q}$	–	rate of heat, heat energy flux, kW
$\dot{Q}_{chem}$	–	chemical energy flux, kW
$\mathbf{t}$	–	total momentum flux
T	–	temperature, K
t	–	temperature, °C
u	–	specific internal energy, kJ/kg
$\mathbf{v}$	–	velocity vector
v	–	specific volume, m^3/kg
V	–	volume, m^3
$\dot{V}$	–	volume flow rate, m^3/s
$W_d(LHV)$	–	lower heating value, kJ/kg
x	–	vapour quality
X_m	–	volumetric fraction of the m component of mixture, m^3/m^3
Y_m	–	mass fraction of the m component of the mixture, kg/kg
z	–	height, m
∂V	–	the contact area of the solid structure with the working medium
0D	–	zero-dimensional algebraic model of flow based on integral balances of mass, momentum and energy
3D	–	three-dimensional model based on differential equations, which requires complete geometry of a flow channel
$\otimes$	–	dyadic multiplicator
ASU	–	air separation unit
WCC	–	wet combustion chamber
CSE	–	spray-ejector condenser
C	–	compressor
GT	–	gas turbine
HE	–	heat exchanger
G	–	electric generator
M	–	motor
CHE	–	cooling heat exchanger
P	–	pump

Greek symbols

β	–	coefficient of enhancement energy conversion
γ	–	volumetric fraction of component in the mixture of the component, kg/m^3
Δp	–	pressure drop, MPa
ΔT	–	the temperature difference in the heat exchanger, K
ζ	–	flow losses for changing diameter channel
η	–	efficiency
κ	–	isentropic coefficient
π	–	pressure ratio
Π_s	–	the dimensionless compression ratio
Π_{cav}	–	the dimensionless cavitation ratio
ρ	–	density, kg/m^3
τ	–	viscous stress tensor
φ	–	velocity coefficient
χ	–	the volumetric entrainment ratio
χ_m	–	the mass entrainment ratio

Subscripts and superscripts

a	–	air
BC	–	Brayton cycle
C	–	compressor
CC	–	combustion chamber
DBC	–	double Brayton cycle
din	–	diffuser nozzle
e-e	–	cross section of primary nozzle
ex	–	exhaust
el	–	electrical
f	–	fuel
g	–	generator
GT	–	gas turbine
i	–	internal
in	–	point in inversed Brayton cycle
IBC	–	inverted Brayton cycle
m	–	mechanical
o-o	–	cross section of secondary nozzle
RE	–	regenerative heat exchanger
s	–	isentropic
s-s	–	cross section of suction section
t	–	technical
t-t	–	cross section of diffuser section
TIT	–	turbine inlet temperature
1s,2s,...	–	isentropic points of process
1,2,...	–	real points of process
$\alpha =$	–	e-e, o-o, s-s, t-t cross sections

1 Introduction

In conventional steam or gas-steam power plants one of the larger devices operating in the thermodynamic cycle is the steam condenser. Its proper operation not only affects the cooling system of the cooling water pumps, but also involves the appropriate expansion in the turbine [1–6]. In turn, in this work, the condenser is a device which, in addition to maintaining a sufficient level of vacuum, should ensure the compactness of the structure. This reduction in size is possible by shortening the vapor condensation path, which does not need to flow over a dozen rows of pipes to cool down and then condense [7] but, by direct mixing with cooling water there, is an immediate volume condensation. Solutions of spray condensers became known already long time ago [8] as well as the direct heat exchanger using steam condensation on injected water [9]. However, in this paper we focus on the system using the ejector. An example of a system that connects the ejector with condenser as well as CO_2 and water separator is shown in Fig. 1. This system should be called the spray-ejector condenser. These are following elements of the ejector: supply chamber (E), power supply (motive) nozzle (A), delivery nozzle (B), mixing chamber (C), diffuser (D), suction chamber (S). There are following characteristic working cross sections:

- the outlet cross section of the supply nozzle with a characteristic cross-sectional area A_{e0}
- mixing chamber 2-3 with cross-section A_m
- diffuser 3-t.

At the beginning, it is also worth mentioning that the spray-ejector condenser can be considered as a device preferred for the enhancement of energy conversion, a phenomenon that improves the exchange of mass, momentum, and energy, starting with the primary nozzle, where the motive fluid, due to the turbulators in the circumferential direction, receives enormous kinetic energy [10,11]. As a consequence, at the edges of the turbulator are formed local discontinuities of flow and disrupts the integrity of the stream, i.e., voids at a pressure much lower than the liquid saturation pressure. Disintegration of liquids into droplets also occurs, and then, as a result of the destruction of continuous carrier, the internal energy and the enthalpy of the liquid stream can be converted into kinetic energy and surface tension energy. Thus, the flow of liquid leaves the cross-section of the surface primary nozzle A_{e0} in the form of discrete potential drops having enormous peripheral velocity $c_{\varphi 0}$ and axial velocity c_{a0}.

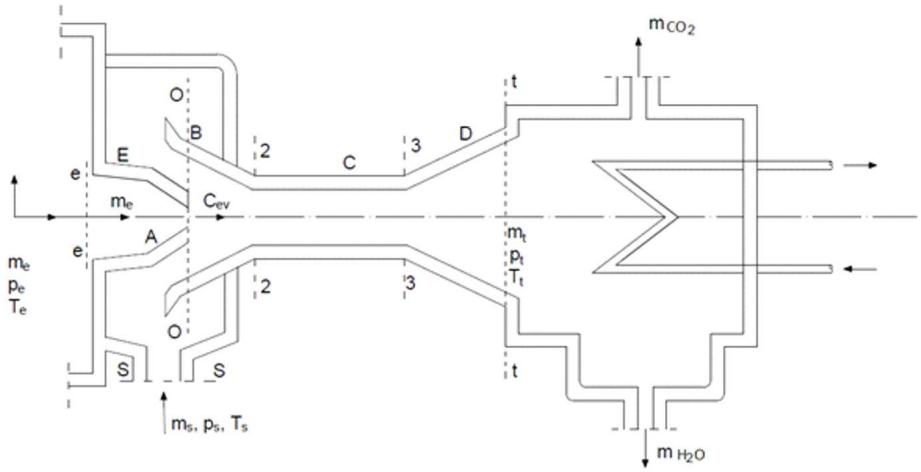

Figure 1: The scheme of the spray-ejector condenser, where E is the supply chamber, A – primary nozzle, B – secondary nozzle, C – mixing chamber, D – diffuser, S – suction chamber. Parameters of the working fluid: cross section e–e : $\dot{m}_e$ – mass flow rate, T_e – temperature, $\rho_e = \rho_{water}$ – density of the working fluid, p_e – static pressure, cross section s-s $\dot{m}_s$ – mass flow rate, T_s – temperature, $\rho_s = \rho_{gs}$ – density of suction gas mixture, p_s – static pressure of suction gas, cross section t-t, $\dot{m}_t$ – mass stream, T_t – temperature, $\rho_t = \rho_{gt}$ – density of the mixture, p_t – static pressure of mixture gas, $\dot{m}_{H2O}$ – water mass flow rate, $\dot{m}_{CO2}$ – carbon dioxide mass flow rate.

Entering the catching nozzle (B), the dispersed stream of propellant fluid can, in principle, behave like free stream, which does not interact with the surrounding gas stream in the inlet [12,13]. In fact, there are many phenomena of small scale [14–17] observed in nanoliquid or nanochannels:

- Further decomposition of the drive stream (pulverization–spraying) governed by inertia, supercooling, surface friction, and surface tension of both linear and curved droplets [18].
- Centrifugal rejection of the largest droplets outside the stream and enlargement of the cross-section of discrete stream to the catching nozzle dimensions, and further disintegration of droplets to the dimensions of the nucleation points.
- Transferring the kinetic energy of the propulsion stream to the suction stream through a viscous change of droplet and gas momentum based on the surface mechanism (Duhem, Navier, and Du Buat numbers) [19–20].
- Transparent transfer of kinetic energy of the propulsion stream (imagined as

a stream of equivalent nanodrops) to the suction gas. In these phenomena, Reynolds thermal transpiration and Graham's component transpiration are important [17,21].

- Thermal transfer of kinetic energy in Smoluchowski's thermal jumping mechanism occurs between relatively cold droplets and a warm gas medium [22–23].
- Diffusion transfer of the kinetic energy of the droplet exchanging the mass with the surroundings on the basis of the Levis mechanism [24].

The transfer of kinetic energy, carried by the sprayed (injected) drive fluid to the suction gas, is thus a complex phenomenon in which various mechanisms interweave. This process further occurs in the mixing chamber which, having a constant cross section, neither accelerates nor slows the mixing of the two streams. Its length is most often determined experimentally and chosen so that the phenomena have time to equalize the propulsion potential–hence the stream of mixture exiting out the mixing chamber should be homogeneous.

Further conversion of the kinetic energy of the mixture into the energy of its compression is effected in a 3-t outlet diffuser where the stream is slowed down and the initial separation of the components finally takes place in the outlet chamber of the spray-ejector condenser. There is a substantial increase in outlet pressure to the value of p_t. The diffuser operating as a flow speed reduction instrument depends to a large extent on the homogeneity of the velocity field in cross-section 3-3. Studies clearly show that in diffuser (D) with an angle of openings $\alpha \sim 10^\circ$ it is possible to recover up to 80% of the compressive energy [25–27].

2 Thermodynamic processes in two-phase ejector

Three-component two-phase liquid-gas ejector is a device in which the liquid is used for compression, partial condensation and pushing the gas medium. In the case of this cycle, we could use even a three-component ejector, as the vapor is mixed with CO_2. In our case, the driven liquid is circulating water with the parameters of about 4 MPa and a temperature of 298 K. The gas is a two-component mixture of water vapor and CO_2 coming from the low-pressure part of the gas-steam turbine. The main feature of this device, unlike blowers and compressors, is the absence of metal moving surfaces in which, usually, the medium gets the power that converts into compressive and kinetic energy [28,29]. Unlike conventional condensers, there is not a huge amount of steam condensation in the device, as condensation occurs directly on the nano-drops.

Typically, the flow of gas in the ducts of power equipment is fixed, for example, the gas flows from high pressure areas to lower pressure areas (turbines, valves, pipelines, nozzle, reactors) or from lower pressure areas to higher pressure areas (pumps, compressors, fans) [10,24,28–45]. In mentioned devices mainly one-phase flow occurs, for example: in gas turbine [29,31,39,41,43,45], high pressure steam turbine [33,36,38,42], water turbine [40]. However, two-phase flow is characteristic for last stages of steam turbine [32,35,37] or steam condenser [30,34,44]. The ejector is a flow device in which the flow of medium occurs simultaneously in two directions, as shown in Fig. 2 [26,27,46–70]. Ejectors have a wide range of medium flowing in the mixture [26], nevertheless, for spray - ejector condenser two-phase occurs. In a classic two-phase ejector, the motive medium (most often water) circulates and is circulated, while its temperature within a relatively short time after startup is adjusted to the temperature of the sucking gas [26,55–58]. In this work, the motive medium is cooled and has a constant temperature of about 298 K, hence the temperature difference always occurs as an additional driving medium both for flow and condensation.

The operating principles of the liquid-gas ejector requires a lower pressure region, p_0, at the outlet of the nozzle (0-0) than in the cross section *s-s*. The suction gas mass flow rate, $\dot{m}_s$, increases as the result of the pressure difference increase, namely: p_0 – static pressure of water in cross section 0-0 and p_s – static pressure of suction gas (see Fig. 1). The suction gases stream, $\dot{m}_s$, possess much lower total kinetic energy than outlet stream, $\dot{m}_t$, and only a small fraction of the kinetic energy of the motive gases stream, $\dot{m}_e$, is converted into compression work. This process of energy conversion in liquid-gas ejector strongly depends on the nozzle design [26,27,48].

On the other hand, in order to treat the flow as a whole there must be a pressure difference between the inlet and the outlet: $p_e > p_t$. This means that the flow channel of the feed stream must be shaped in such a way that the pressure drop $p_e - p_t$ is not a steady linear drop but is a more instantaneous pressure decrease p_0 to $p_0 < p_s$. If, due to a specially shaped drive nozzle, an area for the destruction of the liquid jet at pressure p_0 is formed, the suction gas will flow from the high pressure area $p_s > p_0$ to the lower pressure area p_0. To improve the operating ejector: $p_0 \leq p_s \leq p_t \leq p_e$. In practice, there are encountered high-pressure liquid-gas ejectors $\pi_{ts} = p_t/p_s > 30$. The pressure ratio $\pi_{es} = p_e/p_s$ can range from 100 to 10 [26,27,48].

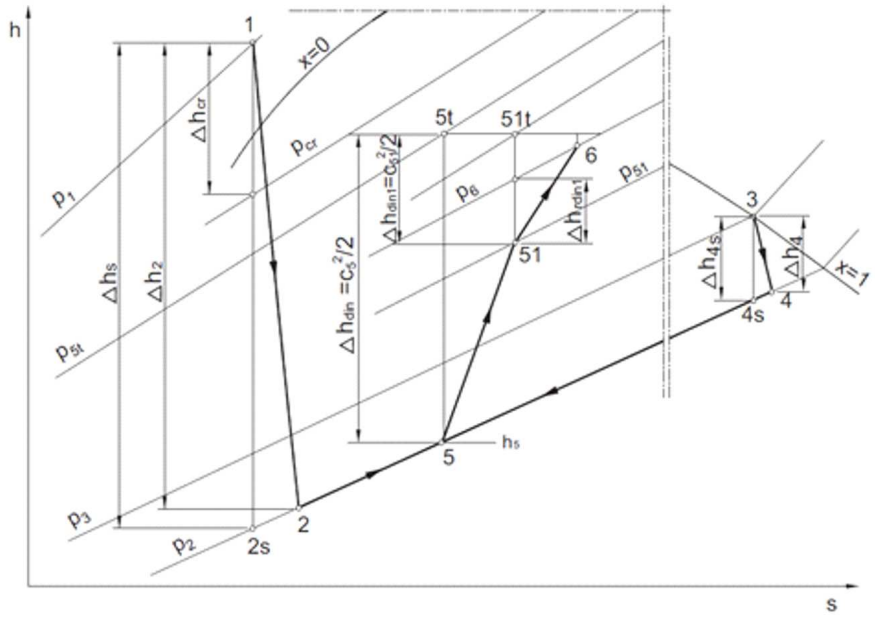

Figure 2: Transitions occurring in a liquid-gas ejector, where 1–2 primary flow acceleration and expansion, 1–2s primary flow isentropic acceleration and expansion, 3–4 secondary flow expansion, 3–4s secondary flow isentropic expansion, 2–5 and 4–5 isobaric mixing in the mixing chamber, 5–51 pseudo shock wave process, 51–6 compression in the subsonic diffuser, $\triangle h_s$ – isentropic enthalpy difference of the primary flow acceleration and expansion, $\triangle h_2$ – enthalpy difference of the primary flow acceleration and expansion, $\triangle h_{cr} = c_{cr}^2/2$ – critical enthalpy difference of the primary flow acceleration and expansion, c_{cr} – the sound velocity at the primary nozzle critical cross-section, $\triangle h_{4s}$– isentropic enthalpy difference of the secondary flow expansion, $\triangle h_4$ – enthalpy difference of the secondary flow expansion, $\triangle h_{din} = c_5^2/2$ – enthalpy difference equal to the kinetic energy at the end of the momentum transfer process in the mixing chamber (upstream of the pseudo shock wave), $\triangle h_{din1} = c_{51}^2/2$ – enthalpy difference equal to the kinetic energy of the combined flow downstream of the pseudo shock wave, $\triangle h_{rdin1}$ – enthalpy difference resulting in a pressure rise in a subsonic diffuser; $x = 0$ – saturated liquid, $x = 1$ – saturated vapour [27,49].

3 Integral characteristics of the device

Figure 1 presents a diagram of the construction of a liquid-gas ejector as a spray – ejector condenser with a water-carbon dioxide separator. Based on this drawing, the integral parameters describing the efficiency of the liquid-gas ejector will be defined. The main characteristics of the liquid-gas ejector are the dependence of

the dimensionless compression ratio, Π, on the volumetric entrainment ratio, χ. In principle, the mass entrainment ratio, χ_m, could be distinguished by a relatively large difference between the motive and the suction mass flow rate:

$$\chi_m = \frac{\dot{m}_s}{\dot{m}_e}\,. \tag{1}$$

Due to such a large disparity between the mass flow supplying to power the ejector, $\dot{m}_e$, and the mass flow rate suction by ejector, $\dot{m}_s$, the volumetric entrainment ratio, χ, is also expressed by

$$\chi = \frac{\dot{V}_s}{\dot{V}_e}\,. \tag{2}$$

Both mass and volumetric entrainment ratio, mainly: χ_m and χ, respectively, means quotient produced by the division of flow rate suction by flow rare ejected. In this sense, the entrainment ratio is the ratio of the suction flow rate to the motive flow rate and its value depend on the ejector type. Typically for the liquid-gas ejector, the mass entrainment ratio obtains value equal from $\sim 10^{-4}$ to $\sim 10^{-3}$, however the volume entrainment ratio is higher, mainly: from $\sim 10^{-1}$ to about 7. Another important parameter is the energy efficiency of the liquid-gas ejector, which is defined as the ratio of the compressive power added to the energy of the supplied power stream

$$\eta_e \ = \frac{N_s}{\dot{E}_e}\,, \tag{3}$$

where $N_s = \ \dot{m}_s(h_{16} - h_{15})$ is as compressive power, $\dot{E}_e = \dot{m}_e[u_e + \frac{p_e}{\rho_e} + z_e g + \frac{1}{2}\left(c_{ae}^2 + c_{\varphi e}^2\right)]$ denoted available energy stream of ejections, u_e – internal energy, p_e – static pressure in cross section e-e, ρ_e – density in cross section e-e, z_e – height in cross section e-e, c_{ae} – axial velocity component, and $c_{\varphi e}$ - circumferential velocity component in cross-section e-e. The literature also makes reference to the work done separately on the gas and on the fluid

$$\eta_{SEC} \ = \frac{N_{ss}}{\dot{E}_e}\,, \tag{4}$$

where $N_{ss} = \ \dot{m}_{sg} l_{2,3g} + \dot{m}_{sH2O} l_{2,3}$ is the work performed by compressed gas and pumped water. This is a definition close to the definition of compressor efficiency in which the work of extracted gas, in the form of kinetic energy of the movable walls, converts in the outlet diffuser into the compressor.

Other basic, dimensionless parameters are [13,26,27,48]:

– pressure ratios

$$\pi_{es} = \frac{p_e}{p_s} , \quad \pi_{et} = \frac{p_e}{p_t} , \tag{5}$$

which correlated with the measurements $\pi_{es} > \pi_{et}$,

– the dimensionless compression ratio

$$\Pi_s = \frac{p_t - p_s}{p_e - p_s} , \tag{6}$$

which can also be expressed by

$$\Pi_s = \frac{\pi_{ts} - 1}{\pi_{es} - 1} , \tag{7}$$

– the dimensionless cavitation ratio

$$\Pi_{cav} = \frac{p_e^c - p_{sat}(T_e)}{p_s^c - p_{sat}(T_e)} , \tag{8}$$

where: $p_{sat}(T_e)$ – the vapor pressure of the liquid at a given temperature; $p_e^c = p_e + \rho_e(c_e^2)/2$ – total pressure at the inlet to the ejector, $p_s^c \approx p_s$ – total pressure in the suction area assuming that the velocity at the inlet to the suction chamber $c_s \approx 0$.

These basic values are calculated by means of direct measurements. Indirect quantities characterizing the ejector are calculated by means of quantities such as pressure p_0 or velocity c_0 in section 0-0. The basic curves used to determine the type of the ejector are [13,26,27,48]:

– the dimensionless compression ratio as a function of the entrainment ratio

$$\Pi_s = \Pi_s(\chi) , \tag{9}$$

– the dimensionless cavitation ratio as a function of the entrainment ratio

$$\pi_{cav} = \sigma_{cr} = \pi_{cav}(\chi) . \tag{10}$$

It should be noted that there are some simple equations describing roughly two-phase ejectors performance, e.g., Sokolov and Zinger proposed the following equation [70]:

$$\frac{1}{\Pi_s} = 2\frac{\varphi_e}{\varphi_s} b \left[\varphi_e \varphi_m \varphi_s - \left(1 - \frac{\varphi_m}{2\varphi_e}\right) b(1+\chi)^2 \right], \tag{11}$$

where: φ_e – velocity coefficient for the primary nozzle, φ_s – velocity coefficient for the suction nozzle, φ_m – velocity coefficient for the mixing chamber, b – constant coefficient. The type of the ejector is also delineated by efficiency characteristics

$$\eta_e = \eta_e(\chi) \, . \tag{12}$$

The utility of integral features is based on their experimental designation [26,51–54]. At present however, among the designers, there are certain principles to be followed in order for the geometry of the ejector to provide proper performance [26,27,48]. In the current state of development of numerical techniques, the calibration of models is becoming more and more common with regard to experimental characteristics [46,50,55–60]. Thus it can be concluded that the development of computational fluid dynamics (CFD) modelling allows for obtaining a characteristic number, which would be significantly similar to the measurement, e.g., 20%. However, to describe the basics of both 3D and 0D models, it is necessary to present the basics of classical phenomenological models that are derived from experimental observations.

4 The basics of phenomenological models

In general, the mixing process of the components combined with the condensation of one of them involves the simultaneous transfer of mass, momentum, and thermal energy between two streams. But even in a particularly simple case where mixing streams have the same temperature and pressure, the mixing process in the flow is extremely complex. Due to the specifics of geometry and parameters, it has become common to distinguish three different mechanisms that determine if the ejector works like a compressor even in the case of isothermal mixing. These are the mechanisms discovered by classical experimentation:

- Witte – shock mixing [61,62],
- Darcy-Weisbach – friction mixing [52,57],
- Flügel-Cunningham – pulse mixing [63,64].

Shock mixing takes place with negligible low kinetic energy of the vortex movement and is caused by the inhibition of the stream in the inlet of the mixing chamber and then in the change of the annular flow into the fog flow (foam) which returns against the flow center. Before the shock mixing zone the gas is in a continuous phase while the liquid in this zone is the continuous phase and the gas is dispersed in the form of bubbles. In the shock mixing zone, in a small section of the mixing chamber, the pressure jump [61,62] and the mixing zone moves, purely oscillating with the flow. Witte's zero-dimensional shock mixing model is based on the flat shock waveform model of compressible fluid, and its main feature is the omission of friction and viscosity as a factor influencing the transfer of energy to the supplying power stream of the suction stream. In front of the shock mixing zone, there is a difference in velocity between the liquid and gaseous phase, which is also due to the difference in kinetic energy of both streams. Beyond the shock mixing zone the whole kinetic energy difference converts into the compression of the mixture and the kinetic energy of the mixture is below the average kinetic energy of the streams before mixing. This model is relatively simple to implement in 0D computational flow mechanics (CFM) codes[1].

Biswas and Mitra friction mixing is based on experiments and devices where the process of transferring kinetic energy from the liquid to gas phase takes place using turbulators mixing both streams, and the equalization of the speed of both components is stretched within the space of the device [52]. However, the shape of the first nozzle seems to be the most important factor of the turbulence process [65–68]. The friction mixing mechanism favors one-dimensional models of two-phase flows in which there is a slippage between the phases [55,60,71]. This velocity slip is described by the additional differential equations, developed in the last quarter of the last century [19–21,71], but also takes into account the implementations of numerical codes more sophisticated boundary conditions [17,21,72,73].

Flügel-Cunningham pulse mixing , unlike the two previous stationary mechanisms, is a pulsed mixing mechanism based on dynamic phenomena occurring within the gripping nozzle and the mixing chamber [63,64]. The essence of this mechanism is pulsatile compression of the gas occurring in the form of a 'plug' occupying the entire cross section of the mixing chamber. Compression water is here in the form of a movable gas-engaging piston. In the pulsed movement of the piston ('water plug') the kinetic energy is directly converted into the compressed gas. In other words, Flügel-Cunningham's mechanism assumes that the process

[1]Computation flow mechanics (CFM) is the contemporary method of simultaneous solving flow governing equations for integrated, so-called 0D description of unknowns parameters of the power plant apparatus

of mixing in a liquid-gas ejector involves simultaneous compression and acceleration of the compressed gas stream so that single bubbles are driven into the drive liquid region [69].

5 The balance of momentum and energy in the ejector

Engineering, zero-dimensional calculations of stationary operation of a liquid-gas ejector and other flow mechanisms are based on algebraic models of mass, momentum and energy balance [30,74,75]. The ejector has two inlets and one outlet, and as the basic boundary conditions they are presented below.
Parameters of the motive fluid, cross-section e-e:

- $\dot{m}_e$ – water mass flow rate,
- T_e – temperature,
- $\rho_e = \rho_{water}$ – density of working liquid,
- p_e – static pressure.

Parameters of the suction fluid: cross section s-s:

- $\dot{m}_s$ – gas mixture mass flow rate,
- T_s – temperature,
- $\rho_s = \rho_{gs}$ – density of suction gas mixture,
- p_s – static pressure of suction gas.

The density of the suction gas mixture, ρ_{gs}, takes the simplest form:

$$\rho_{gs} = X_{H2O}\rho_{H2O} + X_{CO2}\rho_{CO2} = X_{H2O}\rho_{H2O} + (1 - X_{H2O})\rho_{CO2} \ , \tag{13}$$

where ρ_{gs} is the density of the mixture of water vapor and carbon dioxide, X_{H2O} [m^3 vapor/m^3 of the mixture] represents the volumetric fraction of water vapor in the mixture, ρ_{H2O}, ρ_{CO2} [kg of the component/m^3 of the component] is the individual density of the component determining the mass of the component relative to the unit of volume occupied by this component. In more general terms, the density of a mixture, that is, the mass of the components relative to the unit of volume of the mixture [kg of mixture/m^3 of mixture], is:

$$\rho = \sum_{m=1}^{NS} X_m \rho_m \ , \tag{14}$$

where X_m is the volume fraction [m^3 of the m component/m^3 of the mixture], while ρ_m is the density of the component [kg of the component/m^3 of the component]. Density of the mixture can be defined as:

$$\rho = \frac{1}{\sum\limits_{m=1}^{NS} \frac{Y_m}{\rho_m}} , \tag{15}$$

where Y_m is the mass fraction [kg of the m component/kg of the mixture]. Equations (14) and (15) show that the sum of mass fractions and volume fractions equals unity, as follows:

$$\sum_{m=1}^{NS} Y_m = 1 , \qquad \sum_{m=1}^{NS} X_m = 1 . \tag{16}$$

If X_m is volumetric fraction [m^3 component/m^3 of mixture], mass fraction of components will be

$$Y_m = \frac{W_m}{\overline{W}} X_m , \tag{17}$$

where, in turn, X_m takes values $0 \leq X_m \leq 1$, while for $X < 1$ the mixture is unsaturated and for $X = 1$ is saturated. $\overline{W}$ [$\frac{\text{kg}}{\text{mol}}$] is the average molecular weight and W_m [$\frac{\text{kg}}{\text{mol}}$] is the molecular weight of the m component.

Parameter $X_{(s)H2O}$ at the inlet s-s is the resultant from the combustion and expansion processes in the wet combustion chamber and the turbine. On the other hand, parameter $X_{(t)H2O}$ at the outlet in section t-t should be reduced by the amount of vapor that has condensed between the section s-s and t-t

$$\Delta X_{H2O} = X_{(s)H2O} - X_{(t)H2O} , \tag{18}$$

where X_{H2O} is related to the volume of the mixture, assuming that the feed water stream only breaks down into primary drops and does not evaporate. Unlike other engineering modelling mechanisms, the ejector, even though we do not know its final dimensions, requires the determination of the kinetic energy and the length of the vector velocity, usually denoted by the letter c. 0D modelling of ejector in stationary working condition consists of solving three-dimensional equations of momentum and scalar equation of energy in the area with a power supplying inlet e-e, suction inlet s-s and outlet t-t to the final condenser cooling system, and appropriate walls and characteristic cross-sections such as 0-0, 1-1, 2-2 cross

sections, Fig. 1.

The basic reference parameter is the velocity of motive fluid c_{ea}, calculated as if there was no suction medium, hence it was assumed $\dot{m}_s = 0$. This is an abstract quantity in which the index e denotes motive liquid and index a denotes the extreme condition ($\dot{m}_s = 0$) and is calculated as follows:

$$c_{ea} = \varphi_{ea}\sqrt{2\Big(\frac{p_e}{\rho_e} - \frac{p_s}{\rho_s}\Big)}\,, \tag{19}$$

where the velocity coefficient $\varphi_{ea} \approx 0.95$–$0.99$. This comparative velocity is also called Flügel velocity [26] and allows determination of other cross-sectional speeds: c_{e0}, c_{s0}, c_2 or c_t.

The most important is the velocity of the outlet cross-section of the motive nozzle, c_{e0}, corresponding to the pressure drop $p_e - p_0$. Assuming the pressure p_0, then the velocity of the outlet cross-section of the motive nozzle from balance is approximately:

$$c_{e0} = \varphi_{e0}\sqrt{2\Big(\frac{p_e}{\rho_e} - \frac{p_0}{\rho_e}\Big)}\,, \tag{20}$$

where $\varphi_{e0} = 0.92$–0.95. However, in the case of a high value of inlet velocity in the motive nozzle c_{e-e} this variant should be defined by

$$c_{e0} = \varphi_{e0}\sqrt{2\Big(\frac{p_e}{\rho_e} - \frac{p_0}{\rho_e}\Big) + c_{e-e}^2}\,, \tag{21}$$

while the flow rate of the gas mixture in the ring cross-section A_{s0}, corresponding to the pressure drop $p_s - p_0$ in typical case equals

$$c_{s0} = \varphi_{s0}\sqrt{2(i_s^0 - i_{s0})}\,, \tag{22}$$

where $\varphi_{s0} = 0.92$–0.95 and $i_s^0 = i_s^0(T_s, p_s, X_s)$ is the enthalpy of the suction mixture gas (cross-section s-s – Fig. 1), $i_{s0} = i_{s0}(p_0, T_0)$ enthalpy of the suction mixture in cross-section 0-0 and area of cross-section A_{s0}. However, in the case of the spray-ejector condenser when water first cools and then condenses the steam from the mixture, the enthalpy drop should be considered as a phase change and it is not able to accelerate working fluid. Hence, the inlet velocity of suction gases into the mixing chamber should be considered as

$$c_{s0} = \varphi_{s0}\sqrt{2\Big(\frac{p_{s-s}}{\rho_{s-s}} - \frac{p_{o-o}}{\rho_{s-o}}\Big) + c_{s-s}^2}\,. \tag{23}$$

Furthermore, in the case of spray-ejector condenser, when the mixture fully condenses in the mixing chamber, the enthalpy drop should also be considered as a phase change and the velocity at the inlet to the diffusor can be defined as:

$$c_3 = \varphi_{MC} \frac{(c_{s-o}\dot{m}_s + c_{e-o}\dot{m}_e)}{\dot{m}_s + \dot{m}_e} \ . \tag{24}$$

Mass, momentum and energy balance of the device in the analysis region e-e, s-s, t-t equals:

$$\dot{m}_e + \dot{m}_s = \dot{m}_t \ , \tag{25}$$

$$\dot{m}_e \mathbf{c}_e + p_e A_e \mathbf{n}_e + \dot{m}_s \mathbf{c}_s + p_s A_s \mathbf{n}_s - \mathbf{R}_{e0} - \mathbf{R}_{s0} - \mathbf{R}_{0t} = \dot{m}_t \mathbf{c}_t + p_t A_t \mathbf{n}_t \ , \tag{26}$$

$$\begin{aligned} \dot{m}_e\Big(u_e + \frac{p_e}{\rho_e} + z_e g + \frac{c_e^2}{2}\Big) + \dot{m}_s\Big(u_s + \frac{p_s}{\rho_s} + z_s g + \frac{c_s^2}{2}\Big) \\ -\dot{m}_e \Delta e_{e,0} - \dot{m}_s \Delta e_{s,0} - \Delta E_{0m} + \dot{m}_s l_{2,3} - \dot{m}_t \Delta e_{0,t} \\ = \dot{m}_t\Big(u_t + \frac{p_t}{\rho_t} + z_t g + \frac{c_t^2}{2}\Big) \ , \end{aligned} \tag{27}$$

where: $\dot{m}_e \Delta e_{e,0}$ – energy losses of flow in the channel between e-e and 0-0, $\dot{m}_s \Delta e_{s,0}$ – energy losses of flow in the channel between s-s and 0-0, $\dot{m}_t \Delta e_{0-t}$ – energy losses of flow in the channel between 0-0 and t-t , ΔE_{om} – loss of mixing that takes into account the phase change occurring in the shock wave area [26,27].

This can be expressed in words as [30,74]:

- the motive liquid mass flow rate added to the mass flow rate of the suction mixture is equal to the mass flow rate of the mixture exiting the ejector;
- the flux of momentum of the motive working fluid increased by the momentum flux of the suction working fluid, reduced by the loss of momentum, is equal to the momentum flux of the mixture leaving the ejector;
- the total energy flux of the motive fluid, increased by the total energy of the suction fluid, reduced by the loss of energy and increased by the compressive operation, is equal to the total energy flux of the mixture exiting the ejector.

The above balances were derived for stationary flows without simplifying the corresponding 3D expressions, hence the above equations were defined:

Mass flow rate:

$$\dot{m}_\alpha = \iint_{A_\alpha} (\rho_\alpha) \mathbf{v}_\alpha \mathbf{n}_\alpha dA_\alpha \ , \quad \alpha = e, s, t \, , \tag{28}$$

taken as working fluid from the mass flow rate in the cross-section A_α where $\mathbf{v}_\alpha$ is the velocity vector, ρ_α – density, $\mathbf{n}_\alpha$ – unit vector normal to the section. Cross-section area, A_α, does not have to be a cylindrical or spherical surface. The formula above makes it easy to move from 3D to 0D calculations and to compare with 0D measurements.

Fluxes of momentum:

$$\dot{m}_\alpha \mathbf{c}_\alpha + p_\alpha A_\alpha \mathbf{n}_\alpha = \iint_{A_\alpha} (\rho_\alpha \mathbf{v}_\alpha \otimes \mathbf{v}_\alpha + p_\alpha \mathbf{I}) \mathbf{n}_\alpha dA \,, \quad \alpha = e, s, t \,, \tag{29}$$

where vector of the mean velocity $\mathbf{c}_\alpha$ is expressed as follows:

$$\mathbf{c}_\alpha = \frac{\iint_{A_\alpha} \rho_\alpha \mathbf{v}_\alpha (\mathbf{v}_\alpha \, \mathbf{n}_\alpha) dA}{\dot{m}_\alpha} \,, \tag{30}$$

where: p_α – mean pressure in cross-section α, while the average normal vector $\mathbf{n}_\alpha$ is perpendicular to the cross surface in the center of pressure.

Energy fluxes

$$\dot{m}_\alpha \Big(u_\alpha + \frac{p_\alpha}{\rho_\alpha} + z_\alpha g + \frac{c_\alpha^2}{2} \Big) = \iint_{A_\alpha} \rho_\alpha \Big(u_\alpha + \frac{p_\alpha}{\rho_\alpha} + z_\alpha g + \frac{1}{2} \mathbf{v}_\alpha \, \mathbf{v}_\alpha \Big) \mathbf{v}_\alpha \, \mathbf{n}_\alpha dA \,, \alpha = e, s, t, \tag{31}$$

where: u_α – mean specific internal energy of the mixture, $z_\alpha g$ – mean gravity energy, $\frac{c_\alpha^2}{2}$ – mean kinetic energy, $\frac{p_\alpha}{\rho_\alpha}$ — mean compressive energy.

The most difficult elements of 0D modelling include closures to friction force and mobility

$$\mathbf{R}_{\alpha,0} = \iint_{A_{\alpha,0}} (\boldsymbol{\tau} + \mathbf{R} + \mathbf{D} + \mathbf{f}_{\partial V} \otimes \mathbf{n} + \mathbf{n} \otimes \mathbf{f}_{\partial V}) \mathbf{n} dA; \; \alpha = e{-}0, \; s{-}0, \; 0{-}t, \tag{32}$$

where dissipational members are: $\boldsymbol{\tau}$ – the flux of viscous stress, $\mathbf{R}$ – Reynold's turbulent flux, $\mathbf{D}$ – momentum flux resulting from the diffusion, and a general form of boundary forces $\mathbf{f}_{\partial V}$, that consist of contributions from the friction and the mobility components: $\mathbf{f}_{\partial V} = \mathbf{f}_r + \mathbf{f}_m$. Based on integration inside channels the dissipational members can be expressed as energy losses as follows:

- $\dot{m}_e \Delta e_{e,0}$ – in channel between e-e and 0-0,
- $\dot{m}_s \Delta e_{s,0}$ – in channel between s-s and 0-0,
- $\dot{m}_t \Delta e_{0-t}$ – in channel between 0-0 and t-t,

- ΔE_{om} – loss of mixing that takes into account the phase change occurring in the shock wave area [26,27].

Expression $\mathbf{f}_{\partial V} \otimes \mathbf{n} + \mathbf{n} \otimes \mathbf{f}_{\partial V}$ describes the overlapping phenomena with regard to the transfer of kinetic energy of the propulsion stream to the suction stream through the viscous exchange of droplet and gas momentum based on the surface mechanism (Duhem, Navier, and du Buat numbers) [19,20]. As mentioned above, transpiration effects can be seen here, and then the kinetic energy of the propulsion stream (imagined as a stream of equivalent nanodroplets) will be transferred to the suction gas. In these phenomena, Reynolds thermal transpiration and Graham's component transpiration are important especially in the area so called enhancement energy conversion [17,21]. There is still the open issue of modelling thermodynamic effects on the surface interphase. How much these effects influence the observed enhancement energy conversion is not clear and are still developing.

There is a separate issue of closure for the work of compression in the mixing channel $\dot{m}_s l_{2,3}$. Cunningham for gas mixtures [26] calculates the work of the compressor based on the pressure increase in the compression chamber

$$l_{2,3} = \frac{\dot{m}_{sg}}{\dot{m}_t} RT_0 \ln\left(\frac{p_3}{p_0}\right) + \frac{\dot{m}_{sH2O}}{\dot{m}_t} v_0 (p_3 - p_0) \; . \tag{33}$$

Missing closures

For calculation, the internal pressure and temperature are needed 0-0, 2-2, 3-3. Due to the proximity of the sections 0-0 and 2-2 it can be assumed that there exist the same pressures and temperatures. The missing magnitudes in the equations of momentum and energy are presented as follows:

Mean velocities:

$\mathbf{c}_e = c_e \mathbf{e}_x = \dot{m}_e / \rho_e A_e \mathbf{e}_x$ – inlet velocity of the motive liquid,

$\mathbf{c}_s = c_s \mathbf{e}_r = \dot{m}_s / \rho_s A_s \mathbf{e}_r$ – inlet velocity of the suction fluid,

$\mathbf{c}_t = c_t \mathbf{e}_x = \dot{m}_s / \rho_t A_t \mathbf{e}_x$ – outlet velocity of the fluid mixture (when ρ_t is known).

Friction forces:

$\mathbf{R}_{e0} = \xi_{e0} \rho_e c_{e0}^2 A_{e-0} \mathbf{e}_x$ – friction force of the motive liquid,

$\mathbf{R}_{s0} = \xi_{s0} \rho_s c_{e0}^2 A_{s-0} \mathbf{e}_r$ – friction force of the suction fluid,

$\mathbf{R}_{0t} = (\xi_{0t} \rho_t c_t^2 + \nu_N c_t) A_{0-t} \mathbf{e}_x$ – friction force of the mixture fluid.

Closures on internal pressures p_0, p_3, and p_t:

$$p_0 = p_s - k_0 \rho_e \frac{c_{e0}^2}{2} \; , \tag{34}$$

$$p_3 = p_0 + k_2 3\rho_s (c_{e0} - c_{s0} - c_3)^2 \ . \tag{35}$$

Closures on internal temperatures:

$$T_{e0} \approx T_e \ , \tag{36}$$

$$T_3 = T_e + \Delta T_{0,3} \ , \tag{37}$$

where $\Delta T_{0,3}$ should be interpreted as a change of temperature due to phase changes occurring in the mixing chamber of the ejector.

In the three balance equations, the basic unknowns are: $\dot{m}_t$, c_t, and T_t. Unknown outlet velocity, c_t, can typically be calculated by unraveling the equation

$$c_t = \varphi_{3,t} \sqrt{2\big[i_3(p_3, T_3) - i_s(p_s, T_s)\big]} \ . \tag{38}$$

However, in the case of the spray-ejector condenser where mixture water with carbon dioxide flows, the process of acceleration should be considered as

$$c_{so} = \varphi_{3,t} \sqrt{2\Big(\frac{p_{s-s}}{\rho_{s-s}} - \frac{p_{o-o}}{\rho_{s-o}}\Big) + c_3^2} \ . \tag{39}$$

6 Analysed cycle

In the first step, the optimal low pressure of double Brayton cycle, with oxycombustion and water injection in the combustion chamber and with a conventional condenser, has been determined to maximize the power output of the steam-gas turbine. The pressure and mass flow rates (fuel, oxygen, and water) of the heat source in the combustion chamber have been given and presented in [76,77]. However, the specifics of the cycle presented in Fig. 3 should be briefly discussed. The dual Brayton cycle consists of a traditional Brayton cycle (BC), points 1–4, and a second inverted Brayton cycle (IBC), points 1in–4in. The term 'inverted cycle' refers to a change of the order of the compressor and the turbine; hence in IBC (Fig. 3)

- firstly, expansion of the medium[2] occurs in the expander gas turbine (GT) (points 1^{in}-2^{in}),
- then regeneration occurs in the heat exchanger (HE) (points 2^{in}–2_a^{in}),
- heat rejection then occurs in the condenser (CON) (points 2_a^{in}–3^{in}),

[2]Medium is the working fluid, mainly a mixture that consists of the products of combustion in a wet combustion chamber (WCC) such as steam and CO_2.

- and finally, compression occurs in the compressor (C) (points 3^{in}–4^{in}) [76,77].

With hot working fluid at atmospheric pressure flowing out of the gas turbine from the Brayton cycle, we could get additional gas turbine power by expanding the exhaust fumes below ambient pressure [76,77]. Thus, this expansion of the gas-steam mixture is similar to the low pressure expansion taking place in the steam turbine. The main disadvantage of the whole system is the necessity for an air-separation unit (ASU), to supply the combustion chamber with pure oxygen. However, the problem of NOx emission is almost entirely eliminated by the 95% oxy combustion. Additionally, a nitrogen turbine (GTN2) could be utilised and would be fuelled by nitrogen from the oxygen and nitrogen separation station (ASU) [23].

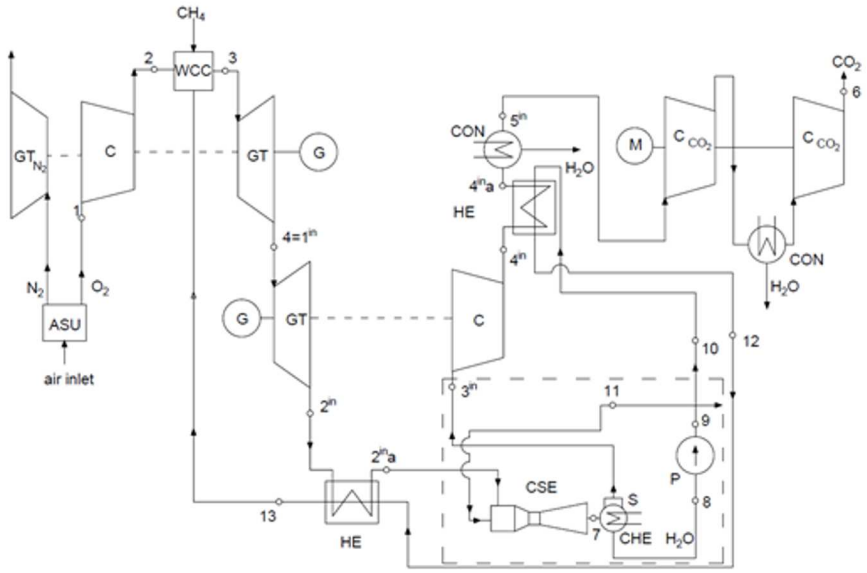

Figure 3: Schematic diagram of the steam-gas cycle with use enhancement energy conversion: ASU – air separation unit, WCC – wet combustion chamber, CSE – spray-ejector condenser, C – compressor, GT – gas turbine, HE – heat exchanger, G – electric generator, M – motor, CHE – cooling heat exchanger, P – pump, GTN2 – additional gas turbine of N_2, C_{CO_2} – compressor of CO_2, S – gas-water separator. Cold sub-cycle with spray-ejector condenser is marked in the dashed frame.

The calculations of the heat cycle have been performed for the constant mass flow rate of: oxygen $\dot{m}_{O2} = 51.8$ kg/s; water $\dot{m}_{H2O} = \dot{m}_{11} = 117.7$ kg/s; fuel $\dot{m}_f = 12.83$ kg/s at the combustion chamber inlet. The total exhaust mass flow

rate is approximately $\dot{m}_{ex} = 182.3$ kg/s. The combustion chamber pressure was also fixed at 4 MPa. Moreover, the temperature difference in the heat exchanger HE was also assumed to be $\Delta T = 30$ K. Additionally, the condensation temperature was assumed to be $t_3^{in} = 30\,^{\circ}\mathrm{C}$ [76,77]. The main innovation of the present steam-gas cycle, which is shown in Fig. 3, in comparison to the cycle presented in works [76,77] occurs in the enhanced condensation which is based on nanoinjection of the cold water condensate and a jet-powered compression of CO_2 performed in the spray-ejector condenser (CSE) [10,11]. This device – CSE is the most important part of the cold subcycle (marked in dashed frame in Fig.3), which additionally consists of a gas-water separator (S, 7-3^{in}), the low pressure cooling heat exchanger (CHE, 7-8) and the pump (P, 8-9). Due to the compactness of the combustion chamber with oxycombustion and water cooling by thermal transpiration and additionally the direct spray-ejector condenser, enhanced energy conversion is to be obtained. After the condenser CSE, the working fluid is cooled (CHE) and then separated from water and CO_2 in the separator (S).

The main aim of the spray-ejector condenser is the separation of CO_2 and steam while simultaneously condensing steam and compressing CO_2 from 8 to 100 kPa. It should be mentioned that the gas-steam mixture (exhaust gases – water) leaving the gas turbine is of a high temperature; therefore, it requires cooling in a special heat exchanger (exhaust gases – water), in which water is warming up and is then injected into the combustion chamber (CC). After being cooled, the exhaust emissions go to the spray-ejector condenser (CSE) in which the steam component of steam-gas is condensed – the amount of condensed water depends on the final expansion pressure. Because the gas pressure is lower than the atmospheric pressure (point 2_a^{in}), the pressure is raised through use of a diffusor and it dries the exhaust (CSE+S) in subsequent devices. The schematic diagram of the cold subcycle has been presented in Fig. 4, highlighting the most important points of the spray-ejector condenser. Furthermore, a pressure-enthalpy diagram of the spray-ejection condenser thermodynamic processes has been illustrated in Fig. 5. Important information is revealed by the method of modelling the phase transformation between points 2_a^{in}-11b (see Figs. 4 and 5). Mixing of water from point 11a with the mixture of gases from point 2_a^{in} in the condenser space where water droplet type condensation occurs. This process of volumetric direct immediate condensation is shown in Figs. 4 and 5. Heat transfer between the two fluids is described by equation

$$\dot{m}_{2^{in}}(h_{2_a^{\in}} - h_{11b}) = \dot{m}_{11}(h_{11b} - h_{11a})\,, \tag{40}$$

where $\dot{m}_{11}$ is few times larger than the water mass flow rate required for full condensation of water from point 2_a^{in}. So the 11b point must not lay on saturation

line $x = 0$ (see Fig. 5). It can be said that the distance between the saturation line and point 11b determines χ_m, which is a parameter similar to the circulation rate of cooling water in the conventional steam condenser. However, the value of χ_m should provide the accurate level of the volumetric entrainment ratio χ, mainly $\chi \approx 1$, which is typical for appropriately designed water-gas ejectors. It should connote the proportion of gases in mixture in point 2_a^{in}, which can be summarised as

$$\dot{m_2^{in}} = Y_{CO2}\dot{m}_{2^{in}} + Y_{H2O}\dot{m}_{2^{in}} \ , \tag{41}$$

where $Y_{CO2} = 0.193$ and $Y_{H2O} = 1 - Y_{CO2}$ [76]. In a way similar to that described in Eq. (41), volumetric decomposition can be defined as

$$\dot{V}_{2^{in}} = X_{CO2}\dot{V}_{2^{in}} + X_{H2O}\dot{V}_{2^{in}} \ , \tag{42}$$

where $X_{CO2} = 0.09$ and $X_{H2O} = 1 - X_{CO2}$ [76].

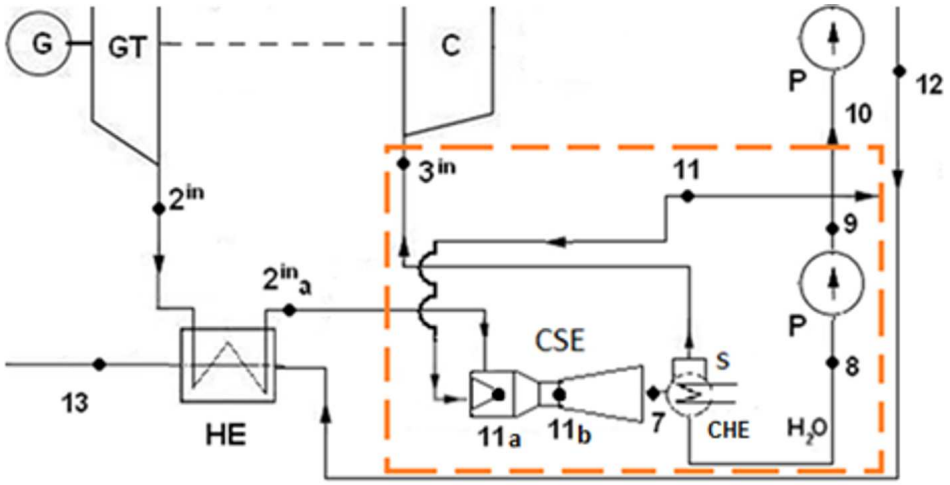

Figure 4: Schematic diagram of cold subcycle with spray-ejector condenser highlighting the most important points.

7 Assumptions and results

The general reason for the application of the ejector in the compression system in the afore discussed configuration (see Fig. 5) is the possible direct condensation of steam and an increase in the pressure ahead of the compressor in the inverse Brayton cycle (or eliminating the compressor of that inverse Brayton cycle). To

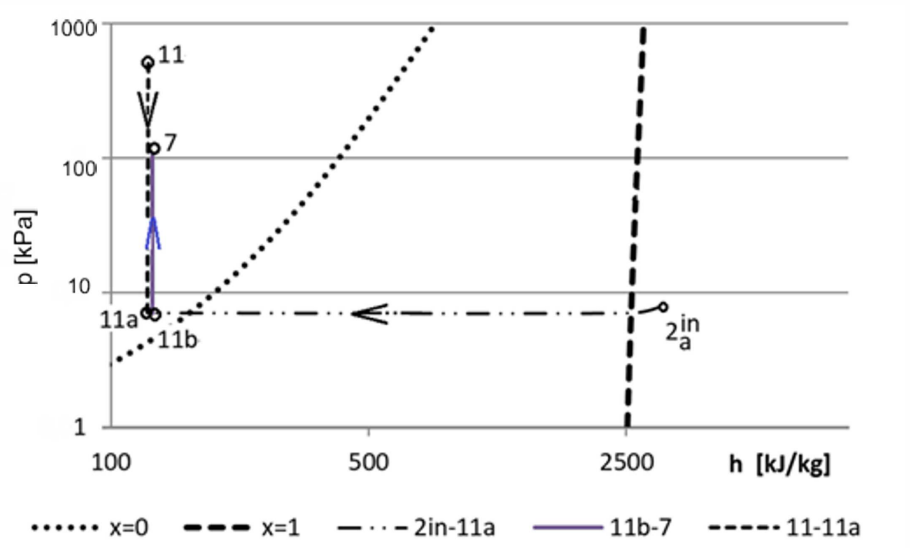

Figure 5: Pressure–enthalpy diagram of the spray-ejector condenser thermodynamic processes.

analyse the double Brayton cycle with oxy-combustion and capturing of the CO_2, the CFM code was used. Mathematical CFM models use mass, momentum and energy equations in the 0D engineering form [23,30,31,74,78]. In previous paragraphs computational procedures for each component of the spray-ejector condenser were proposed. Additionally, governing equations of other devices in the turbo assembly are defined [30,74,76,78], namely: the compressor, the combustion chamber, the turbines, the pumps and the heat exchangers [78–82]. It should be mentioned that CFM code has been developed also in the area of steam cycles [79,81], gas cycles [81,83], combined cycles [84], organic Rankine cycles [79,81], carbon capture and storage systems and other configurations [76,85], taking into account the efficiency of the whole power plant [78–85]. However, mathematical procedures at the design level have been used for many years and still cannot be replaced by other approaches, which has been confirmed in many publications [78–85].

For this analysis the following equations have been implemented. The electrical efficiency of the whole system, $\eta_{el-netto}$, is defined as a quotient of the electrical power, N_{el}, generated by the block and chemical energy flux, $\dot{Q}_{chem}$, contained in the fuel

$$\eta_{el-netto} = \frac{N_{el}}{\dot{Q}_{chem}} = \frac{N_{el}}{\dot{m}_f W_d} \,, \tag{43}$$

where $\dot{m}_\rho$ is the fuel mass flow rate and W_d is the lower heating value. The efficiency of the Brayton cycle, η_{el-BC}, may also be given as a quotient of the electrical power, N_{el-BC}, and the chemical energy flux contained in the fuel

$$\eta_{el-BC} = \frac{N_{el-BC}}{\dot{m}_f W_d} \,. \tag{44}$$

However, the double Brayton cycle efficiency is defined as a quotient of the electrical power, N_{el-DBC}, generated by the double Brayton cycle and fuel chemical energy flux contained in the fuel

$$\eta_{el-DBC} = \frac{N_{el-DBC}}{\dot{Q}_{chem}} \,. \tag{45}$$

The efficiency of the inversed Brayton cycle η_{el-IBC} is described as a difference between the η_{el-DBC} and η_{el-BC} as is shown below

$$\eta_{el-IBC} = \eta_{el-DBC} - \eta_{el-BC} \,. \tag{46}$$

In [76] the results of analysis showed that despite an initial decrease in traditional Brayton cycle efficiency η_{el-BC}, the total block efficiency η_{el-DBC} increased due to the decrease in condensation pressure. For example, the efficiency of the inverted Brayton cycle increased to a value of $\eta_{el-IBC} = 15.3\%$ at a condensing pressure of around $p = 7$ kPa. The optimal efficiency value $\eta_{el-netto}$ for the entire block was identified as being at a pressure of $p = 7.7$ kPa in the condenser. This value may rise due to increased flow in the wet combustion chamber. Additionally, the whole system efficiency falls by around 8.66% due to the production of oxygen (6.38%) and the capture of CO_2 (2.28%).

The mentioned parameters have been stated as referential points for the thermodynamic analysis of the cold subcycle. The results along with the data for the accurate points in the optimal efficiency have been published in [76]. However, additional information for the thermodynamic analysis of the spray-ejector condenser was necessary, mainly: the dimensionless compression ratio, Π_s, the volumetric entrainment ratio, χ, axial velocity component, $c_{a\alpha}$, area of cross section, A_α, velocity coefficient, φ_α, and others of less importance.

One of the mentioned parameters was the velocity of the working medium between the outlet of the turbine and the inlet to the condenser, mainly in the turbine exhaust hood. An optimal geometric design of the exhaust hood is typically achieved through multiple design iterations in conjunction with computational methods estimating the performance of every such design [87–88]. Use of

the total pressure, mass flow rate and velocity boundary conditions at the inlet to spray-ejector condenser are evaluated for inlet boundary modelling. In addition, a comprehensive study of inlet velocities with respect to their ability to predict the pressure loss is reported in many papers [87–90].

A recommendation on the values of inlet velocities for condenser modelling is arrived at the level equals $\mathbf{c}_{s-s} = 50$ [1] and 100–200 [87–88]. So as high speeds are not typical for ejectors, this simulation should be treated as a theoretical analysis. Also the values of velocity in a motive nozzle should be proportionally larger in comparison to the recommended data, namely 10–50 m/s. Furthermore, the mentioned speed has been assumed to be at the level 100 m/s. The thermodynamic parameters of the medium at the characteristic points of the cold subcycle are presented in Tab. 1, as where inlet parameters assumed for point 2_a^{in}.

The efficiencies of devices assumed for different operating conditions determined the following values:

0.80 for the isentropic efficiency of the motive nozzle,
0.80 for the isentropic efficiency of the suction nozzle,
0.95 for the mixing efficiency of the mixer,
0.05 for the mixing loss friction factor of the mixer,
0.70 for the isentropic efficiency of the diffuser.

Table 1: The thermodynamic parameters of the medium at the characteristic points of cold subcycle for the condenser inlet pressure at the level of $p_{2_a^{in}} = 7.8$ kPa.

Point	t [C]	p [kPa]	c [m/s]	h_c [kJ/kg]	h [kJ/kg]	$\dot{m}$ [kg/s]	$\dot{V}$ [m^3/s]	A [m^2]	ρ [kg/m^3]
$2_{a^{in}}$	302.0	8	50.00	1.25	3080.79	182.3	5216.8	104.34	0.03494
$2_{s^{in}}$	39.0	7	559.19	156.35	2571.76	182.3	1773.9	3.17	0.10277
11	15.0	500	100.00	5.00	126.20	145332.3	145.9	1.46	995.82
11_a	15.0	7	104.84	5.50	125.75	145332.3	145.9	1.39	995.82
11_b	15.9	7	100.13	5.01	129.48	145514.6	146.2	1.46	995.33
7	15.9	105	99.14	4.91	129.66	145514.6	146.2	1.47	995.37

The data in Tab. 1 were obtained for the dimensionless compression ratio $\Pi_s = 0.199$, the volumetric entrainment ratio $\chi = 1.09$, velocity in a suction chamber $c_{s-s} = 50$ m/s, and axial velocity component in motive nozzle $c_{e-e} = 100$ m/s.

The most interesting result is the value of the velocity in suction chamber,

which attains transonic value with Mach number approx. 1.2, occurs as the result of density change. This phenomena is common for nozzles in the last stages of steam turbines [90], for the air-foils [91], and experiments with the Laval nozzle [92], and are considered to have a negative influence on working these devices [91,93] because it causes noise and vibration [94]. However, as was already mentioned, the normal shock wave which should take part in compression process in mixing chamber within the ejector can also occur [27,49,51,57] (see Fig. 1). Taking into account the location of shock wave propagation, mainly based on Tab. 1. within the suction chamber, the velocity of the fluid can accelerate the condensation processes however it does not increase the pressure of fluid. Hence, compression is conducted only in the diffuser of the spray ejector-condenser.

As was presented in Fig. 5. and Tab. 1 the outlet pressure from the spray-ejector condenser was fixed at the level 100 kPa. The thermodynamic parameters of the medium in the characteristic points of the cold subcycle for the condenser inlet pressure at the level of $p_{2_a^{in}} = 7.8$ kPa have been collected in Tab. 1. The output power and the efficiency calculations of cycles with the spray-ejector condenser are also defined in the present paper as

$$\eta_{el-CSE} = N_{el} - N_{CSE}\dot{Q}_{chem} \, , \tag{47}$$

where the electrical power of the pump in the cold subcycle N_{CSE} can be represented by the following relationship:

$$N_{CSE} = \dot{m}_{11}\nu_{11}(p_{11} - p_7) = \dot{V}_{11}(p_{11} - p_7) \, . \tag{48}$$

The numerical analysis has shown that the total energy output decreases as the cold subcycle is being used. The net efficiency of the double Brayton cycle with the spray-ejector condenser has reached the value of $\eta_{el-CSE} = 37.78\%$ for the parameters presented in Tab. 1. The decrease in the efficiency is caused by the consumption of electrical power by the pump of motive water which must be pumped to the spray ejector-condenser. So the drop of efficiency is equal to 5.91%. However, there is still open question which value of the volumetric entrainment ratio should be considered for modelling the thermodynamic effects on the spray-ejector condenser. How far these calculation are treated, as they are preliminary and are still under development.

There are logical circumstances to speak with respect to enhanced energy conversion in the spray-ejector condenser. The phase transformation which occurs on the surface of droplets can be characterised by the surface phenomena of increasing area density in volume. Additionally, velocities reached in the spray-ejector

condenser are higher by about an order of magnitude in comparison to a conventional steam condenser. To estimate the value of enhanced energy conversion for power plants, a coefficient should be introduced

$$\beta_{el} = \frac{N_{el}}{V_{el}} , \tag{49}$$

where N_{el} is the electrical power generated by the block and V_{el} is a cubature of the power plant. The value of this coefficient describes the density of electrical energy. However, in the classic papers [95,96] it is well known that the inverse parameter, which, takes into account the dimensions of the power plant, and is referred to as the specific cubature of the main building of the power plant. Some preliminary calculations for the development of the coefficient of enhanced energy conversion was presented in [97]. Based on [97] the value of β_{el} was estimated also for conventional power plants $\beta_{el} = 0.1$–5 kWel/m^3 as well as for the third generation gas power plant $\beta_{el} = 10$–500 kWel/m^3. Speaking about the spray ejector-condenser, the rate of heat transfer from the hot mixture of exhaust gases and cooling water should be considered. Hence another coefficient should also be considered, mainly enhanced energy conversion for heat transfer, which in the literature, addressing heat transfer [98–102] is referred to as the volumetric heat flux density

$$q = \frac{\dot{Q}}{V} , \tag{50}$$

where $\dot{Q}$ is the heat flux and V is the cubature of the devices. The typical value of the volumetric heat flux density equals $q = 180$ kWt/m^3. In the case of the spray ejector-condenser this volumetric heat flux density can amount to $q_{CST} = 5800$ kWt/m^3 hence an increase of about 32 times. On the basis of this calculation, it can be stated that in the spray ejector-condenser occurs an enhanced energy conversion for heat transfer.

8 Conclusions

Engineering (zero-dimensional) calculations of the stationary operation of a liquid-gas ejector and other flow machines are based on algebraic models of mass, momentum and energy balance. However, using the mentioned codes, prediction of the most important parameters like power and efficiency of the thermodynamic systems is possible. The obtained efficiency of the double Brayton cycle with the spray-ejector condenser amounts to about $\eta_{el-CSE} = 37.78\%$. The drop in

efficiency is equal to 5.91 point of percentage in comparison to a cycle with a conventional steam condenser, however the proposed innovation of the discussed cycle provides an increase of about 32 times the volumetric heat flux density.

The discussed system, considering a compact, zero-emission gas-steam turbine should contain small-sized devices, for example: 1) a wet combustion chamber (with oxy-combustion and use of cooling water transpiration), 2) a spray-ejector condenser (using bulk condensation on the surface of steam-gas water droplets). Hence, the results of the thermodynamic analysis indicates the legitimacy of building cycles based on an enhanced energy conversion.

Acknowledgments The author gratefully acknowledges his supervisor, Professor Janusz Badur, for his scientific support and advice during the article's preparation. The author also would like to thank Mr Richard Sitkiewicz-Batten for English corrections.

Received in July 2017

References

[1] Trela M., Butrymowicz D., Matysko R.: *Diagnostic of flow and thermal processes in power plant heat transfer equipment*. In: Diagnostics of New-Generation Thermal Power Plants, Edits: (T.Chmielniak, M.Trela, Eds.) Wydawnictwo IMP PAN, Gdańsk 2008, 339–402.

[2] Badur J., Kowalczyk T., Ziółkowski P., Tokarczyk P., Woźniak M.: *Study of the effectiveness of the turbine condenser air extraction system using hydro ejectors*. Trans. Inst. Fluid-Flow Mach. **131**(2016), 41–53.

[3] Butrymowicz D., Trela M.: *Problems of condensation heat transfer in power plant heat exchangers*. Trans. Inst. Fluid-Flow Mach. **113**(2003), 107–118.

[4] Salij A., Stępień J.: *Operation of the Turbine Condensers in Thermal Power Plants*. Kaprint Publishers, Lublin 2013 (in Polish).

[5] Strušnik D., Golob M., Avsec M.: *Effect of non-condensable gas on heat transfer in steam turbine condenser and modelling of ejector pump system by controlling the gas extraction rate through extraction tubes*. Energ. Convers. Manage. **126**(2016), 228–246.

[6] Trela M., Ihnatowicz E., Krupa A., Najwer M., Banasiewicz J.: *Monitoring of air content in air-vapour mixture removed from power plant condensers*. Trans. Inst. Fluid-Flow Mach. **114**(2003), 219–228.

[7] Marto P.J., Nunn R.H.: *Power condenser heat transfer technology: Computer Modelling/Design/Fouling*. Hemisphere Publishing Corporation, Washington 1981.

[8] Heeren H., Visarius I.: *A spray condenser*. Patent specification 59149/1968r. Polish Patent Office, 31.01.1970 (in Polish).

[9] De Paepe M., Dick E.: *Technological and economical analysis of water recovery in steam injected gas turbines*. Appl. Therm. Eng. **21**(2001), 135–156.

[10] Ziółkowski P., Zakrzewski W., Badur J.: *Innovative thermodynamical cycles based on enhancement mass, momentum, entropy and electricity transport due to slip, mobility, transpiration, entropy and electric jumps as well as other nano-flows phenomena*. In: Proc. 12th Joint European Thermodynamics Conf. JETC2013 (M. Pilotelli, G.P. Beretta, Eds.), Brescia 2013, 482–487.

[11] Badur J.: *Development of Energy Concept*. Wyd. IMP PAN, Gdańsk 2009 (in Polish).

[12] Sobieski W.: *Jet pumps – numerical modelling possibilities upon the bifurcation phenomena*. Techn. Sci. **13**(2010), 240–255. DOI 10.2478/v10022-010-0023-6.

[13] Sobieski W.: *Modelling of mixing phenomenon and cavitation occures in gas-fluid ejector*. PhD thesis, Gdańsk 2002 (in Polish).

[14] Badur J., Karcz M., Lemański M., Nastałek L.: *Foundation of the Navier-Stokes boundary conditions in fluid mechanics*. Trans. Inst. Fluid-Flow Mach. **123**(2011), 3–55.

[15] Badur J., Karcz M., Lemański M.: *On the mass and momentum transport in the Navier-Stokes slip layer*. Microfluid Nanofluid **11**(2011), 439–449.

[16] Ziółkowski P., Badur J.: *On Navier slip and Reynolds transpiration numbers*. CNM 2017, 5th Conference on Nano- and Micromechanics, 4-6th July 2017, Wrocław, Poland

[17] Badur J., Ziółkowski P.: *Further remarks on the surface vis impressa caused by a fluid-solid contact*. In: Proc. 12th Joint European Thermodynamics Conf. JETC2013, (M. Pilotelli, G.P. Beretta, Eds.), Brescia 2013, 581–586.

[18] Badur J., Ziółkowski P.J., Ziółkowski P.: *On the angular velocity slip in nano flows*. Microfluid Nanofluid **19**(2015), 191–198.

[19] Ziółkowski P., Badur J.: *On the Boussinnesq eddy viscosity concept based on the Navier and du Buat number*. In: Appl. Mech. 2014 Sci. Sess., Book of Abstracts. (Sawicki J., Ed.), Bydgoszcz 2014, 87–88.

[20] Ziółkowski P., Badur J.: *Navier number and transition to turbulence*. J. Physics: Conf. Ser. **530**(2014), 012035. DOI:10.1088/1742-6596/530/1/012035.

[21] Ziółkowski P., Badur J.: *On the unsteady Reynolds thermal transpiration law*. J. Physics: Conf. Ser. **760**(2016), 012041. DOI:10.1088/1742-6596/760/1/012041.

[22] Badur J., Ziółkowski P., Zakrzewski W., Sławiński D., Kornet S., Kowalczyk T., Hernet, J., Piotrowski R., Felincjancik J., Ziółkowski P.J.: *An advanced Thermal-FSI approach to flow heating/cooling*. J. Physics: Conf. Ser. **530**(2014), 012039. DOI:10.1088/1742-6596/530/1/012039.

[23] Ziółkowski P., Badur J.: *A thermodynamic and technical analysis of a zero-emission power plant in Pomerania*. Techn. Trans., Mechanics **3**(2017), 197–210. DOI: 10.4467/2353737XCT.17.042.6353.

[24] Jóźwik P., Badur J., Karcz M.: *Numerical modelling of a microreactor for thermocatalytic decomposition of toxic compounds*. Chem. Process Eng. **32**(2011), 3, 215–227.

[25] Neve R.S.: *Diffuser performance in two-phase jet pumps*. Int. J. Multiphase Flow **17**(1991), 2, 267–272.

[26] Goliński J., Troskaliński A.: *Ejectors Theory and Design*. WNT, Warszawa 1979 (in Polish).

[27] Šarevski V.N., Šarevski M.N.: *Characteristics of R718 refrigeration/heat pump systems with two-phase ejectors*. Int. J. Refrigeration **70**(2016), 13–32.

[28] Perycz S.: *Gas and Steam Turbines*. Wydawnictwo PAN, Wrocław 1992 (in Polish).

[29] Goliński J.A., Jesionek K.J.: *Air-Steam Power Plants*. In: Fluid Flow Machinery (Maszyny przepływowe) (E.S.Burka, Ed.,) Vol. 31, Wydawnictwo IMP PAN, Gdańsk 2009 (in Polish).

[30] Badur J.: *Five lecture of contemporary fluid termomechanics*. Gdańsk, 2005, www.imp.gda.pl/fileadmin/doc/o2/z3/.../ 2005_piecwykladow.pdf (in Polish).

[31] Ziółkowski P., Badur J.: *Clean gas technologies – towards zero-emission repowering of Pomerania*. Trans. Inst. Fluid-Flow Mach. **124**(2012), 51–80.

[32] Kowalczyk T., Kornet S., Ziółkowski P., Badur J.: *Determination of the mass flow rate of multiphase fluids in the classic Venturi measurement nozzle in terms of zero- and three-dimensional calculations*. Current Iss. Energ. Eng. **2**(2014), 135–148.

[33] Puzyrewski R., Biernacki R.: *Volute scroll as an alternative to guide vanes at inlet to a turbine*. Trans. Inst. Fluid-Flow Mach. **114**(2003), 99–110.

[34] Mirzabeygi P., Zhang C.: *Three-dimensional numerical model for the two-phase flow and heat transfer in condensers*. Int. J. Heat Mass Tran. **81**(2015), 618–637.

[35] Kornet S., Badur J.: *Enhanced evaporation of the condensate droplets within the asymmetrical shock wave zone*. Trans. Inst. Fluid-Flow Mach. **128**(2015), 119–130.

[36] Lampart P., Gardzilewicz A., Szymaniak M., Kurant B., Banaszkiewicz M., Malec A.: *Stator blade modification as a method of leakage flow treatment to improve flow efficiency of old-design steam turbine stages*. Trans. Inst. Fluid-Flow Mach. **114**(2003), 19–36.

[37] Zaryankin A.: *Two-tier low pressure cylinders for condensing steam turbines*. Trans. Inst. Fluid-Flow Mach. **126**(2014), 123–130.

[38] Rusanov R., Jędrzejewski Ł., Klonowicz P., Żywica G., Lampart P., Rusanov A.: *Design and performance study of a small-scale waste heat recovery turbine*. Trans. Inst. Fluid-Flow Mach. **133**(2016), 145–162.

[39] Dudda W., Chmiel D.: *Modelling and strength analysis of turbine blades*. Mechanik **7**(2015), 201–208.(in Polish) DOI: 10.17814/mechanik.2015.7.230.

[40] Kaniecki M., Krzemianowski Z.: *CFD analysis of high speed Francis hydraulic turbines*. Trans. Inst. Fluid-Flow Mach. **131**(2016), 111–120.

[41] Piotrowicz M., Flaszyński P., Doerffer P.: *Investigations of shock wave boundary layer interaction on suction side of compressor profile*. J. Physics: Conf. Ser. **530**(2014), 012068 DOI:10.1088/1742-6596/530/1/012068.

[42] Badyda K.: *Mathematical model for digital simulation of steam turbine set dynamics and on-line turbine load distribution*. Trans. Inst. Fluid-Flow Mach. **126**(2014), 65–82.

[43] Flaszyński P., Doerffer P., Szwaba R., Kaczyński P., Piotrowicz M.: *Shock wave boundary layer interaction on suction side of compressor profile in single passage test section*. J. Therm. Sci. **24**(2015), 6, 510–515. DOI: 10.1007/s11630-015-0816-9.

[44] Blaise M., Feidt M., Maillet D.: *Optimization of the changing phase fluid in a Carnot type engine for the recovery of a given waste heat source*. Entropy **17**(2015), 8, 5503–5521. DOI:10.3390/e17085503.

[45] Ochrymiuk T.: *Numerical prediction of film cooling effectiveness over flat plate using variable turbulent Prandtl number closures*. J. Therm. Sci. **25**(2016), 3, 280–286.

[46] Śmierciew K., Butrymowicz D., Kwidziński R., Przybyliński T.: *Analysis of application of two-phase injector in ejector refrigeration systems for isobutane*. Appl. Therm. Eng. **78**(2015), 630–639.

[47] Sumeru K., Nasution H., Ani F.N.: *A review on two-phase ejector as an expansion device in vapor compression refrigeration cycle*. Renew. Sust. Energ. Rev. **16**(2012), 4927–4937.

[48] Trela M., Kwidziński R., Butrymowicz D., Karwacki J.: *Exergy analysis of two-phase steam-water injector*. Appl. Therm. Engi. **30**(2010), 340–346.

[49] Šarevski M.N., Šarevski V.N.: *Preliminary study of a novel R718 refrigeration cycle with single stage centrifugal compressor and two-phase ejector*. Int. J. Refrig. **40**(2014), 435–449.

[50] Banasiak K., Hafner A.: *1D Computational model of a two-phase R744 ejector for expansion work recovery*. Int. J. Therm. Sci. **50**(2011), 2235–2247.

[51] Bhat P.A., Mitra A.K., Roy A.N.: *Momentum transfer in a horizontal liquid-jet ejector*. The Canadian J. Chem. Eng. **50**(1972), 313–317.

[52] Biswas M.N., Mitra A.K.: *Momentum transfer in a horizontal multi-jet liquid-gas ejector*. Canadian J. Chem. Eng. **59**(1981), 634–637.

[53] Neve R.S.: *The performance and modelling of liquid jet gas pumps*. Int. J. Heat Fluid Fl. **9**(1988), 2, 156-164.

[54] Lu X., Wang D., Shen W., Zhu C.: *Experimental investigation characteristics of an interface wave in a jet pump under cavitation condition*. Exp. Therm. Fluid Sci. **63**(2015), 74–83.

[55] He S., Li Y., Wang R.Z.: *Progress of mathematical modelling on ejectors*. Renew. Sust. Energ. Rev. **13**(2009), 1760–1780.

[56] Yuan G., Zhang L., Zhang H., Wang Z.: *Numerical and experimental investigation of performance of the liquid-gas and liquid jet pumps in desalination systems*. Desalination **276**(2011), 89–95.

[57] Banasiak K., Palacz M., Hafner A., Buliński Z., Smołka J., Nowak A.J., Fic A.: *A CFD-based investigation of the energy performance of two-phase R744 ejectors to recover the expansion work in refrigeration systems: An irreversibility analysis*. Int. J. Refrig **40**(2014), 328–337.

[58] Yazdani M., Alahyari A.A., Radcliff T.D.: *Numerical modelling of two-phase supersonic ejectors for work-recovery applications*. Int. J. Heat Mass Tran. **55**(2012), 5744–5753.

[59] Colarossi M., Trask N., Schmidt D.P., Bergander M.J.: *Multidimensional modelling of condensing two-phase ejector flow*. Int. J. Refrig. **35**(2012), 290–299.

[60] Ameur K., Aidoun Z., Ouzzane M.: *Modelling and numerical approach for the design and operation of two-phase ejectors*. Appl. Therm. Eng. **109**(2016), 809–818.

[61] Witte J.H.: *Mixing shocks and their influence on the design of liquid-gas ejectors*. PhD thesis, Uitgeverij Waltman, Delft 1962.

[62] Witte J.H.: *Mixing shock in two-phase flow*. J. Fluid Mech. **36**(1969), 4, 639–655.

[63] Cunningham R.G.: *Gas compression with the liquid jet pump*. J. Fluids Eng. T ASME, **96**(1974), 203–215.

[64] Cunningham R.G., Hansen A.G., Na T.Y.: *Jet pump cavitation*. J. Basic Eng. **92**(1970),3, 483–494.

[65] Rahman F., Umesh D.B., Subbarao D., Ramasamy M.: *Enhancement of entrainment rates in liquid-gas ejectors.* Chem. Eng. Process. **49**(2010), 1128–1135.

[66] Sharma V.P., Kumaraswamy S., Mani A.: *Effect of various nozzle profiles on performance of a two phase flow jet pump.* World Academy of Science, Eng. Technol. **6**(2012), 470–476.

[67] Havelka P., Linek V., Sinkule J., Zahradnik J., Fialova M.: *Effect of the ejector configuration on the gas suction rate and gas hold-up in ejector loop reactors.* Chem. Eng. Sci. **52**(1997), 11, 1701–1713.

[68] Elbel S.: *Historical and present developments of ejector refrigeration systems with emphasis on transcritical carbon dioxide air-conditioning applications.* Int. J. Refrig. **34**(2011), 1545–1561.

[69] Butterworth M.D., Sheer T.J.: *High-pressure water as the driving fluid in an ejector refrigeration system.* Appl. Therm. Eng. **27**(2007), 2145–2152.

[70] Sokolov E.I., Zinger N.M.: *Jet Devices Energoatomizdat.* Moscow 1989 (in Russian).

[71] Biń A.K.: *Gas entrainment by plunging liquid jets.* Chem. Eng. Sci. **48**(1993), 21, 3585–3630.

[72] Badur J., Banaszkiewicz M.: *Model of the ideal fluid with scalar microstructure. An application to flashing flow of water.* Trans. Inst. Fluid-Flow Mach. **105**(1999), 115–152.

[73] Bilicki Z., Badur J.: *A thermodynamically consistent relaxation model for a turbulent, binary mixture undergoing phase transition.* J. Non-Equilib. Thermodyn. **28**(2003), 145–172.

[74] Nastałek L., Karcz M., Sławiński D., Zakrzewski W., Ziółkowski P., Szyrejko Cz., Topolski J., Werner R., Badur J.: *On the internal efficiency of a turbine stage: classical and CFD definitions.* Trans. Inst. Fluid-Flow Mach. **124**(2012), 17–39.

[75] Felicjancik J., Ziółkowski P., Badur J.: *An advanced thermal-FSI approach of an evaporation of air heat pump.* Trans. Inst. Fluid-Flow Mach. **129**(2015), 111–141.

[76] Ziółkowski P., Zakrzewski W., Kaczmarczyk O., Badur J.: *Thermodynamic analysis of the double Brayton cycle with the use of oxy combustion and capture of CO2.* Arch. Thermodyn. **34**(2013), 2, 23–38.

[77] Ziółkowski P., Badur J.: *Selection of thermodynamic parameters in order to improve the environmental performance on the gas-steam turbine cycle.* In: Current Problems of Power Engineering Vol. III (K. Wójs, T. Tietze, Eds.), Oficyna Wydawnicza Politechniki Wrocławskiej, Wrocław 2014, 445–456.

[78] Jesionek K., Chrzczonowski A., Ziółkowski P., Badur J.: *Enhancement of the Brayton cycle efficiency by water or steam utilization.* Trans. Inst. Fluid-Flow Mach. **124**(2012), 93–108.

[79] Ziółkowski P., Kowalczyk T., Kornet S., Badur J.: *On low-grade waste heat utilization from a supercritical steam power plant using an ORC-bottoming cycle coupled with two sources of heat.* Energy Convers. Manage. **146**(2017), 158–173.

[80] Kowalczyk T., Głuch J., Ziółkowski P.: *Analysis of possible application of high-temperature nuclear reactors to contemporary large-output steam power plants on ships.* Polish Maritime Research **23**(2016), 90, 32–41.

[81] Kowalczyk T., Ziółkowski P., Badur J.: *Exergy losses in the Szewalski binary vapor cycle.* Entropy (**17**(2015), 10, 7242–7265. DOI:10.3390/e17107242

[82] Lemański M., Karcz M.: *Performance of lignite-syngas operated tubular solid oxide fuell cell*. Chem. Process Eng. **29**(2008), 233–248.

[83] Ziółkowski P., Piotrowski R., Badur J.: *Accuracy problem of modelling in a gas turbine cycle with heat regeneration according to Szewalskiñs idea*. Trans. Inst. Fluid-Flow Mach. **129**(2015) 77–109.

[84] Bartela Ł., Skorek-Osikowska A., Kotowicz J.: *Thermodynamic, ecological and economic aspects of the use of the gas turbine for heat supply to the stripping process in a supercritical CHP plant integrated with a carbon capture installation*. Energy Conv. Manage. **85**(2014), 750–763.

[85] Skorek-Osikowska A. Bartela Ł., Kotowicz J., Job M.: *Thermodynamic and economic analysis of the different variants of a coal-fired, 460 MW power plant using oxy-combustion technology*. Energy Convers. Manage. **76**(2013), 109–120.

[86] Robinson E.: *Leaving-velocity and exhaust loss in steam turbine.* Fuel Steam Power T ASME **56**(1933), 10, 515-526.

[87] Gardzilewicz A., Świrydczuk J., Badur J., Karcz M., Werner R., Szyrejko C.: *Methodology of CFD computations applied for analyzing flows through steam turbine exhaust hoods*. Trans. Inst. Fluid-Flow Mach. **113**(2003), 157–168.

[88] Veerabathraswamy K., Senthil Kumar A.: *Effective boundary conditions and turbulence modelling for the analysis of steam turbine exhaust hood*. Appl. Therm. Eng. **103**(2016), 773–780.

[89] Tindell R.H., Alston T.M., Sarro C.A., Stegmann G.C., Gray L., Davids J.: *Computational fluid dynamics analysis of a steam power plant low-pressure turbine downward exhaust hood.* , J. Eng. Gas Turb. Power T ASME **118**(1996), 1, 214–224.

[90] Burton Z., Ingram G.L., Hogg S.: *A literature review of low pressure steam turbine exhaust hood and diffuser studies*. J. Eng. Gas Turb. Power, T.ASME, **135**(2013), 6, 062001-062001-10. GTP-12-1424. DOI: 10.1115/1.4023611.

[91] Doerffer P., Szulc O.: *Shock wave smearing by wall perforation*. Arch. Mech. **58**(2006), 6, 543–573.

[92] Kornet S., Badur J.: *Evaporation level of the condensate droplets on a shock wave in the IMP PAN nozzle depending on the inlet conditions*. J. Phys. Conf. Ser. **760**(2016), 012009. DOI:10.1088/1742-6596/760/1/012009.

[93] Szulc O., Doerffer P., Tejero F.: *Passive control of rotorcraft high-speed impulsive noise*. J. Phys. Conf. Ser. **760**(2016), 012031. DOI:10.1088/1742-6596/760/1/012031

[94] Jesionek K.: *Flow separation forecasting and possibility of its reduction in fluid-flow machinery (in turbomachinery)*. Scie. Pap. Insti. of Heat Engi. Fluid Mech. 51, Monographs 28, Wrocław 1998 (in Polish).

[95] Pawlik M., Strzelczyk F.: *Power Plants.* VII Edn., WNT, Warsaw 2012 (in Polish).

[96] Laudyn D., Pawlik M., Strzelczyk F.: *Power Plants.*, III Edn., WNT, Warsaw 1997 (in Polish).

[97] Ziółkowski P., Zakrzewski W., Badur J.: *Innovative thermodynamical cycles based on slip, mobility, transpiration, as well as other nano-flows phenomena*. In: Analysis of Power Engineering Systems (B. Węglowski, P. Duda, Eds.), Warsaw 2013, 351–360 (in Polish).

[98] Bejan A.: *Entropy Generalization Minimization.* CRC Press, Boca Raton 1996.

[99] Bejan A., Kraus A. D.: *Heat Transfer Handbook.* John Wiley & Sons, Hoboken, (published simultaneously in Canada).

[100] Madejski J.: *Theory of Heat Transfer.* Politechnika Szczecińska, Szczecin 1998 (in Polish).

[101] Madejski P., Taler D.: *Analysis of temperature and stress distribution of superheater tubes after attemperation or sootblower activation.* Energ. Convers. Manage, **71**(2013), 131–137.

[102] Wiśniewski S., Wiśniewski T.: *Heat Transfer.* WNT, Warsaw 1994 (in Polish).